

RESEARCH

Open Access



# Disrupted mitochondrial morphology and function exacerbate inflammation in elderly-onset ulcerative colitis

Mengmeng Zhang<sup>1</sup>, Hong Lv<sup>1</sup>, Xiaoyin Bai<sup>1</sup>, Gechong Ruan<sup>1</sup>, Qing Li<sup>2</sup>, Kai Lin<sup>1</sup>, Hong Yang<sup>1\*</sup> and Jiaming Qian<sup>1\*</sup>

## Abstract

**Background** The characteristics of ulcerative colitis (UC) in the elderly are quite different from the young population. Mitochondrial injury is a key mechanism regulating both aging and inflammation. This study aims to reveal the role of mitochondrial damage in the pathogenesis of adult- and elderly-onset UC.

**Methods** RNA-sequencing of colonic mucosa from adult- and elderly-onset UC patients was performed. Mitochondria-related differentially expressive genes (mDEGs) and immune cell infiltration analysis were identified and performed in colonic tissues from UC patients. Mice aged 6–8 weeks and 20–24 months were administered 2% dextran sodium sulphate (DSS) for 7 days to induce colitis. Mitochondrial morphological changes and ATP levels were evaluated in the colons of mice. Mechanistically, we explored the association of key mDEG with reactive oxygen species (ROS), oxygen consumption rates, NLRP3/IL-1 $\beta$  pathway in HCT116 cell line.

**Results** Thirty mDEGs were identified between adult- and elderly-onset UC, which were related primarily to mitochondrial respiratory function and also had significant correlation with different infiltrates of immune cells. Compared with young colitis mice, DSS-induced colitis in the aged mice exhibited more severe inflammation, damaged mitochondrial structure and lower ATP levels in colonic tissues. *ALDH1L1* was identified as a hub DEG through protein–protein interaction networks of RNA-seq, which was downregulated in UC patients or colitis mice versus healthy controls. In tumor necrosis factor-alpha-stimulated HCT116 cells, mitochondrial ROS, NLRP3 and IL-1 $\beta$  expression increased less and mitochondrial respiration had an upregulated trend after knocking down *ALDH1L1*.

**Conclusion** There are significant differences in mitochondrial structure, ATP production and mitochondria-related gene expression between adult- and elderly-onset UC, which have a potential link with cytokine pathways and immune microenvironment. The more prominent mitochondrial injury may be a key factor for more severe inflammatory response and poorer outcome in elderly-onset UC.

## Highlights

1. Aged DSS-induced colitis mice exhibit more severe disrupted mitochondrial morphology, ATP production and more severe inflammation.

\*Correspondence:

Hong Yang

yangh@pumch.cn

Jiaming Qian

qianjm@pumch.cn

Full list of author information is available at the end of the article



© The Author(s) 2025. **Open Access** This article is licensed under a Creative Commons Attribution-NonCommercial-NoDerivatives 4.0 International License, which permits any non-commercial use, sharing, distribution and reproduction in any medium or format, as long as you give appropriate credit to the original author(s) and the source, provide a link to the Creative Commons licence, and indicate if you modified the licensed material. You do not have permission under this licence to share adapted material derived from this article or parts of it. The images or other third party material in this article are included in the article's Creative Commons licence, unless indicated otherwise in a credit line to the material. If material is not included in the article's Creative Commons licence and your intended use is not permitted by statutory regulation or exceeds the permitted use, you will need to obtain permission directly from the copyright holder. To view a copy of this licence, visit <http://creativecommons.org/licenses/by-nc-nd/4.0/>.

2. Elderly-onset UC have significant differences in mitochondria-related molecules expression compared with adult-onset UC.
3. ALDH1L1 expression is significantly increased in elderly-onset UC.
4. ALDH1L1 regulates mitochondrial respiration, mitochondrial ROS, and NLRP3/IL-1 $\beta$  pathways.

**Keywords** Ulcerative colitis, Elderly, Mitochondrial damage, Inflammatory response, Immune infiltration

## Introduction

Ulcerative colitis (UC) is traditionally considered to be prevalent in young adults. However, in recent years, elderly patients with UC are becoming more common [1]. The characteristics of UC in the elderly are quite different from those in the young population. We reported that elderly patients with moderate-to-severe UC present more steroid treatment failure and increased risk of UC-related colectomy, mortality, and severe infections [2]. Therefore, there is a need to identify the mechanisms of “aging-colitis progression” to explain the disease behavior and the poor treatment response in the elderly-onset UC. However, the underlying mechanism of this difference remains unclear. Our previous study found that intestinal barrier dysfunction and gut microbial dysbiosis was more serious in aged mice with dextran sodium sulfate (DSS)-induced colitis than the young mice [3]. Notably, gut barrier integrity and homeostasis rely substantially on sufficient cellular energy, which is mainly supplied by intracellular mitochondria [4]. And several studies have revealed that mitochondrial dysfunction and excessive oxidation are the key factors in the pathogenesis of inflammatory bowel disease (IBD), regulating intestinal epithelial stemness, barrier integrity, innate immunity and gut microbiota [5–7]. Haberman Y et al [8]. demonstrated that by transcriptome sequencing analysis, the expression of genes associated with ATP production or mitochondrial biosynthesis was significantly downregulated in active UC patients, and mitochondrial respiration and activity of electron transport chain complex was also inhibited.

On the other hand, aging is closely associated with cellular energy decline. Due to high energy demands, the human gut is more susceptible to aging [9]. Cellular senescence is always accompanied by mitochondrial alterations, including morphological changes, decreased respiratory function and ATP production, oxidative stress damage [9–11]. “Inflamm-aging” and immunosenescence are another two hallmarks of biological aging, and are characterized by dysfunction of the immune system to pathogens or self-antigens and pro-inflammatory environment [12]. Immune infiltration analysis revealed that a disproportionate number of immune cells from innate and adaptive immune system play critical roles in

some aging-associated diseases [13, 14]. Therefore, we speculate that the interaction between mitochondrial dysfunction and inflammation-immune dysregulation may be an important reason for “aging-colitis progression”. However, the immune infiltration characteristics of elderly-onset UC remains unclear and it is unknown whether mitochondrial alterations during aging increases disease severity through affecting immune function in aged patients with colitis. This study focused on elucidating the relationship between mitochondrial dysfunction and inflammatory response in elderly UC, in order to provide a theoretical basis for disease surveillance in elderly-onset UC and novel interventions to alleviate the inflammatory response or improve drug efficacy from the perspective of mitochondrial function.

Here, this study aimed to elucidate mitochondria-related transcriptomic changes and immune cell infiltration features of elderly-onset UC and comprehensively investigated potential molecular mechanisms involved. Moreover, we conducted DSS-induced colitis mice to further validate the discrepancies in mitochondrial dysfunction between the young and aged mice. These findings provide important insights into the mitochondria-related biological pathways that may predispose elderly patients to UC, suggesting a potential therapeutic approach for treating UC in elderly individuals.

## Methods

### Patients and colonic biopsy

Colonic biopsies from 8 young UC patients and 8 elderly UC patients were performed in this study, and the biopsy site was assessed as endoscopic Mayo score ranging from 2–3. We defined patients diagnosed with UC after 60 years of age as the elderly group, whereas patients with a diagnosis of UC before 40 years of age were defined as the young group. The diagnosis of UC was fulfilled according to the third European Crohn’s and Colitis Organization (ECCO) consensus guidelines [15]. Meanwhile, healthy controls who met the same criteria for age were included, and normal colonic biopsy specimens were collected from these controls. All included cases had no history of comorbidities including malignant tumors, severe hepatic and renal insufficiency, severe cardiovascular and cerebrovascular diseases. Clinical data

and samples were collected after patients signed written informed consent.

### RNA-sequencing analysis and identification of differential genes

Colonic mucosal tissues from 3 young and 3 elderly patients with UC were collected for RNA extraction using RNeasy Plus Mini Kit (Qiagen), followed by RNA-sequencing (RNA-seq) analysis. Library preparation was performed using the NEBNext® Ultra™ RNA Library Prep Kit on an Illumina NovaSeq 6000 platform. HISAT2 (v.2.0.5) was used to map the clean reads to each gene, with raw data normalized to fragments Per kilobase of exon model per million mapped fragments (FPKM) for subsequent analyses. Differentially expressed genes (DEGs) were identified with the DESeq2 (v1.20.0) package with a cutoff of  $P < 0.05$  and  $|\log(\text{fold change})| > 1.0$ , where  $\log_2(\text{FC}) > 1.0$  indicated upregulated genes, and  $\log_2(\text{FC}) < -1.0$  indicated downregulated genes. The DEGs between the young and elderly group were illustrated with a volcano plot generated via the R package “ggpubr”. Functional enrichment analyses of the DEGs were performed with the clusterProfiler package, with the terms of Gene Ontology (GO), Kyoto Encyclopedia of Genes and Genomes (KEGG) and gene set enrichment analysis (GSEA) identified with a cutoff of  $P < 0.05$ .

### Identification of mitochondria-related DEGs and functional enrichment analysis

The Integrated Mitochondrial Protein Index (IMPI) of the MitoMiner database (<http://mitominer.mrc-mbu.cam.ac.uk/>) provides 1626 human mitochondria-related genes. Overlapping genes among DEGs from RNA-seq and mitochondria-related genes from the MitoMiner database were defined as mitochondria-related DEGs (mDEGs). A heatmap of mDEGs expression in adult- and elderly-onset UC patients was drawn based on  $\log_2$ -transformed FPKM values from RNA-seq using the “pheatmap” package in R. Different color indicated the expression of the genes in different samples. As mentioned above, the list of mDEGs was used for GO and KEGG enrichment analyses via the clusterProfiler package.

### Immune infiltration analysis

Based on the RNA-seq results, we further used the CIBERSORT algorithm to evaluate immune cell infiltration and its relationship with mDEGs in adult- and elderly-onset UC. The analysis was performed using the “CIBERSORT” package in R [16]. The FPKM data from RNA-seq was used for the CIBERSORT algorithm. The validated leukocyte gene signature matrix (LM22) was applied to

quantify 22 phenotypes of human infiltrating immune cells (<https://www.nature.com/articles/nmeth.3337#MOESM207>) [17]. The proportions of 22 immune cells in each tissue sample were then calculated. As a reference expression profile of human tissue, the LM22 signature matrix defined 22 infiltrating immune cell components.

A heatmap was generated using R package “pheatmap” to illustrate the proportions of different immune cells in each sample. Comparative analysis of immune cell profiles between adult- and elderly-onset UC tissues was conducted using the Kruskal test, and the results were visualized as the boxplot using R package “ggplot2”. The stacked bar plot figure was generated using R package “ggplot2” to illustrate the composition of 22 immune cell subsets in each sample. We subsequently evaluated the correlations between the proportions of infiltrating immune cells and the 30 mDEGs expression in the adult- and elderly-onset UC group respectively using Spearman’s correlation coefficient with a significance threshold of  $P < 0.05$ . Similarly, the correlation between immune cells was also analyzed. The results were visualized as a correlation heatmap using R package “corrplot”.

### Protein–Protein Interaction (PPI) networks and hub gene identification

A protein–protein interaction (PPI) network of the mDEGs was constructed via STRING (version 12.0), followed by visualization through Cytoscape (version 3.8.2). Then, cytoHubba and MCODE plugins were subsequently used for the identification of gene clusters. The hub gene was identified based on multiple factors including the fold change and significance of differential expression, the degree of connectivity in the PPI network, and subsequent validation of expression in tissue samples.

### Young and aged DSS-colitis mouse model

Male C57BL/6N mice aged 6–8 weeks and 20–24 months, purchased from Vital River Laboratory Animal Technology Co. Ltd. (Beijing, China), were maintained in a specific pathogen-free animal laboratory at a constant temperature of 22°C with a fixed 12-h light–dark cycle. After 1 week of adaptive feeding, the young and aged mice were utilized to establish a colitis model. As we previously reported [3], colitis was induced in mice via the oral delivery of 2% dextran sodium sulfate (DSS) (MP Biomedicals, USA) in drinking water for 7 days. At the end of the treatments, mice were euthanized by cervical dislocation. Deaths of mice not associated with experimental intervention were excluded. All animal procedures were performed in accordance with the guiding principles for the care and use of laboratory animals approved by the Animal Care Committee of Peking Union Medical College Hospital.

During DSS administration, body weight, stool features and hematochezia were recorded daily, and the disease activity index (DAI) was evaluated as previously reported [18], as shown in the Supplementary Material. The mice were sacrificed on day 8, and the length of the colon was measured. The colon tissues were sampled using a Swiss roll technique [19] and fixed in 10% formalin for 48 h and then embedded in paraffin. 4- $\mu$ m slides were stained with hematoxylin and eosin (H&E) for histopathological analysis to assess the pathological score of experimental colitis as previously described [18] (Supplementary Material).

#### Quantitative real-time PCR

The colonic samples collected from patients with UC and DSS-colitis mice were immersed in the RNAlater (ThermoFisher) for RNA extraction. Among these 30 mDEGs, we further selected 14 mDEGs (*HK3*, *DACT2*, *SUGCT*, *ECHDC3*, *ALDH1L1*, *FASTKD1*, *PYCR1*, *HMGCS2*, *TIMM23B*, *TOMM20L*, *MTERF1*, *CLUH*, *PLIN5*, *P2RY12*) that were reported in previous studies (not limited to mitochondrial or inflammation-related studies) and 8 highly reported genes related to NAD(P)<sup>+</sup>/NAD(P)H homeostasis (*ME1*, *ME2*), mitochondrial respiratory complex (*Prkaa2*, *Pdha*, *NDUFS4*, *SDHA*), mitochondrial biogenesis (*PGC1 $\alpha$* , *MFF*) for qRT-PCR. Total RNA was extracted and first-strand cDNA synthesis was performed using FastPure<sup>®</sup> Tissue Total RNA Isolation Kit (Vazyme) and the PrimeScript<sup>™</sup>RT Reagent Kit with gDNA Eraser (Takara). Then, qRT-PCR was performed with TB Green Premix Ex Taq<sup>™</sup>II (Takara). The primer sequences are summarized in Supplementary Table 1 and GAPDH was used as an internal reference. The relative expression of target genes was calculated by the  $2^{-\Delta\Delta C_t}$  method. All PCR reactions were conducted in triplicate.

#### Transmission electron microscopy

Fresh distal colon tissues were fixed with 2.5% glutaraldehyde for 4 h, followed by dehydration in increasing concentrations of ethanol and propylene oxide. The samples were finally embedded in epoxy resin. Ultrathin sections were prepared following standard protocols and mitochondrial morphology was observed with transmission electron microscope (TEM 1400 plus, Japan). Five colonocytes were randomly selected from each sample and the number of mitochondria in each colonocyte was counted manually by 2 investigators blinded to the groups. The average number of mitochondria in each colonocyte was recorded.

#### Assessment of tissue ATP content

Approximately 20 mg of fresh colon tissue was obtained to measure the ATP concentration. According to Enhanced ATP Assay Kit (Beyotime), colon tissue was homogenized and the supernatant was collected to determine the ATP level. The detection solution was added to a 96-well plate and incubated at room temperature for 5 min. The supernatants were then added to the wells and mixed quickly before the luminescence signals were determined via Varioskan Flash (ThermoFisher). Total ATP levels were subsequently calculated on the basis of the luminescence signals.

#### Cell culture and treatment

The human colon cancer cell line HCT-116 was obtained from the American Type Culture Collection (ATCC) and was cultured in RPMI 1640 supplemented with 10% fetal bovine serum (FBS) and 1% penicillin–streptomycin under standard culture conditions (5% CO<sub>2</sub>, 37 °C). HCT116 cells were seeded into 6-well culture plates for 24 h to reach 70–80% confluence, after which the cells were separated into two groups: the non-targeting scrambled control siRNA (NC) group and the ALDH1L1-siRNA (siALDH1L1) group. These reagents were transfected into cells via Lipofectamine<sup>™</sup> RNAiMAX (ThermoFisher scientific) according to the manufacturer's protocol. Following siRNA transfection and 24 h incubation for 24 h, the medium was changed and the cells were treated with TNF $\alpha$  (100 ng/ml) for 24h and collected for RNA and protein extraction. The targeted sequences for the siRNA experiments were as follows: siALDH1L1: 5'-GACCCTCATTCACGGAGATAA -3'; negative control (NC) siRNA: 5'-TTCTCCGAACGTGTCACGT-3'. The efficacy of gene knockdown was validated through qRT-PCR and Western blot analysis (Supplementary Fig. 1).

Tumor necrosis factor (TNF) is a major pathogenic mediator and therapeutic target in IBD, and TNF- $\alpha$  can be used to treat intestinal epithelial cells to induce cellular inflammatory processes, as previously mentioned [20, 21].

#### Mitochondrial ROS detection

Under exogenous TNF- $\alpha$  stimulation, cells treated with siRNAs were assessed for reactive oxygen species (ROS) production with MitoSOX Red (Invitrogen, Cat.no. M36008), a fluorescent superoxide indicator that selectively targets mitochondria. HCT116 cells were stained with 5  $\mu$ M MitoSOX Red for 30 min at 37 °C in a humidified environment with 5% CO<sub>2</sub>. The proportion of MitoSOX-positive cells and the fluorescence intensity were detected via flow cytometry after the cells were washed and suspended.

### Measurement of Oxygen Consumption Rate (OCR)

HCT116 cells transfected with negative non-targeting scrambled control siRNA or ALDH1L1-siRNA were seeded in an XF 24-well cell culture microplate (Seahorse Bioscience, Copenhagen, Denmark) at a density of ( $6\sim7\times 10^4$ ) and incubated overnight, followed by TNF $\alpha$  (100 ng/ml) treatment for 6 h. The hydration of the sensor probe plate and preparation of the mitochondrial stress test kit (Cat.103015–100, Agilent) were then performed according to the manufacturer's recommendations. The final concentrations of oligomycin, the uncoupler carbonyl cyanide-4-(trifluoromethoxy) phenylhydrazone (FCCP), the complex III inhibitor rotenone, and antimycin A (Rot/AA) were respectively 1.5  $\mu$ M, 0.5  $\mu$ M, 0.5  $\mu$ M, respectively. The oxygen consumption rate (OCR) was measured using Seahorse XFe24 extracellular flux analyzer (Agilent, Santa Clara, CA, USA).

### Western blotting

Total protein was extracted from tissue and HCT116 cells treated with siRNA with RIPA buffer (C1053, APPLIED GEN, China), and the protein concentration was determined via BCA protein assay (A53226, Pierce). Loading buffer was added to protein samples, followed by denaturation in a water bath at 100 °C for 10 min. Samples containing the same amount of protein (30  $\mu$ g) were separated with NuPAGE Bis–Tris gels (ThermoFisher). The separated proteins were subsequently transferred to polyvinylidene difluoride (PVDF) membranes. The PVDF membranes were blocked in 5% bovine serum albumin at room temperature and shaken gently for 1 h. Then, the membranes were incubated at 4 °C overnight with primary antibodies diluted with 5% BSA. These primary antibodies included anti-ALDH1L1 (17,390–1-AP, Proteintech, 1:2000), anti-NLRP3 (19,771, Proteintech, 1:1000) and anti-IL1 $\beta$  (12,242, CST, 1:1000) antibodies. The membranes were subsequently washed with Tris-buffered saline-containing tween three times and incubated with appropriate horseradish peroxidase (HRP)-conjugated secondary antibodies at room temperature for 1 h. The protein bands were detected by a chemiluminescence detection system, and GAPDH was used as the internal standard.

### Statistical analysis

Experimental data are expressed as the means  $\pm$  standard errors of the mean (SEMs). The significance of data among the 4 groups was tested using one-way ANOVA test followed by Tukey's multiple comparisons test for normally distributed data, and the Kruskal–Wallis test for nonnormally distributed data.  $P < 0.05$  was considered statistically significant. GraphPad Prism (version 10.0, San Diego, USA) was used for statistical tests, and R (3.6.2, R Foundation for Statistical Computing, Vienna, Austria) was used for data processing and visualization as described above.

### Results

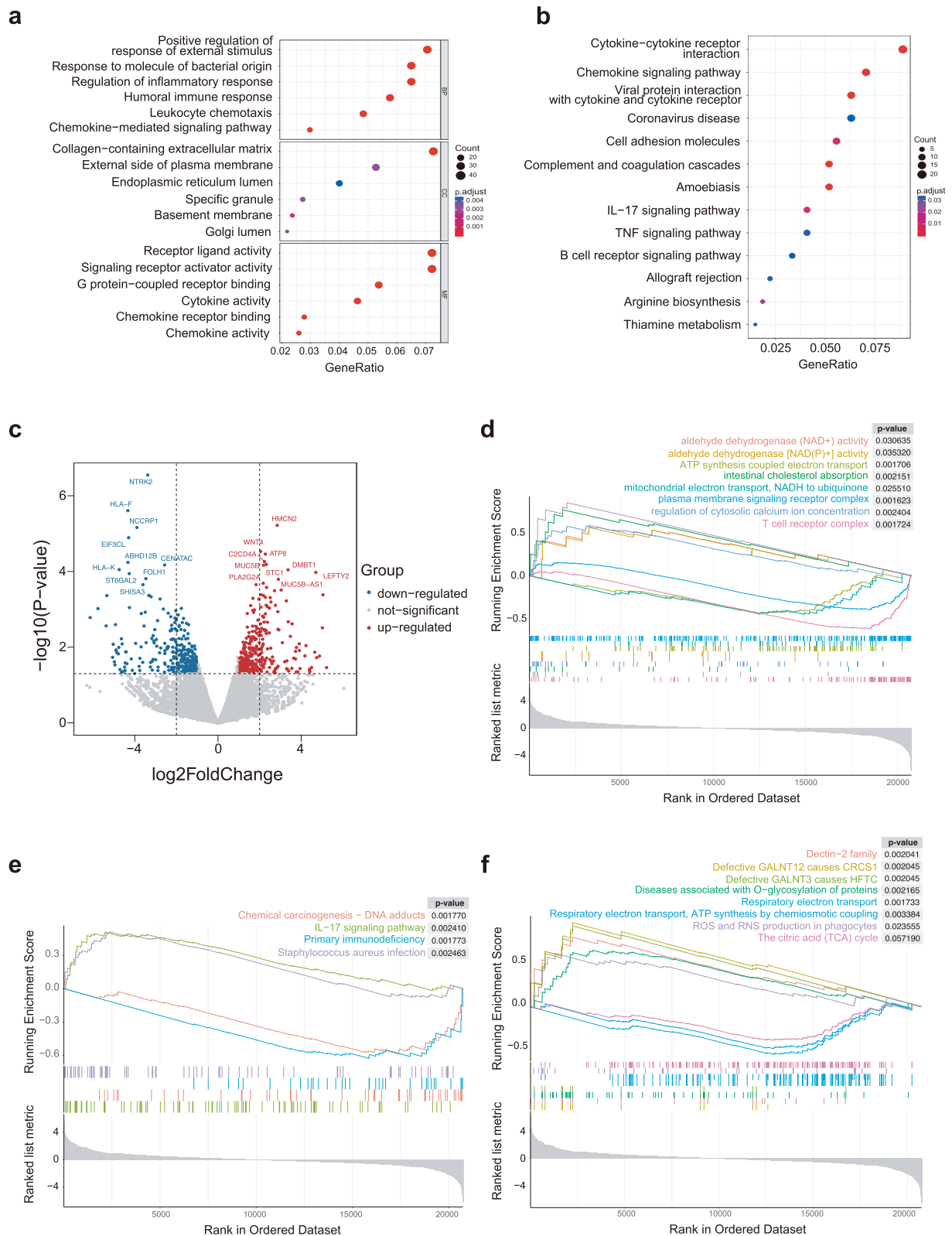
#### Identification of mitochondrial DEGs between adult- and elderly-onset UC and functional enrichment analysis

In this study, transcriptome sequencing was performed with colonic mucosa of 6 UC patients, including 3 adult-onset UC patients and 3 elderly-onset UC patients. There were 713 DEGs between adult- and elderly-onset UC. A volcano plot depicting the distribution of DEGs is shown in Fig. 1c. As is indicated in Fig. 1a, GO biological analysis showed that the DEGs and their encoded proteins were involved in biological processes including the regulation of inflammatory response, immune response, leukocyte chemotaxis, and cytokine activity. And functional analysis of DEGs revealed enrichment in KEGG pathways (Fig. 1b) related to cytokines interaction, chemokine, cell adhesion molecules, TNF signaling pathway, and interleukin (IL-17) signal transduction pathways. GSEA (Fig. 1d, e, f) revealed that, in addition to the T-cell receptor or IL-17 signaling pathways, mitochondria-related pathways, including ATP synthesis, respiratory electron transport, and the NAD(P)<sup>+</sup>/NAD(P)H balance, were also involved ( $P < 0.05$ ).

Subsequently, we identified 30 mDEGs that overlapped with the DEGs identified via RNA-seq analysis and the MitoMiner database. The heatmap, shown in Fig. 2b, represents the 30 mDEGs expression in patients with adult- and elderly-onset UC. As is shown in Fig. 2a, GO functional annotation revealed that the mDEGs and their encoded proteins were mainly related to the mitochondrial outer membrane, oxidoreductase activity and enoyl-CoA hydratase activity. And in Fig. 2a, the enriched KEGG pathways included biosynthesis of amino acids,

(See figure on next page.)

**Fig. 1** The identification and gene-set enrichment analysis of differentially expressed genes (DEGs) between adult- and elderly-onset UC patients. **a.** GO analysis of DEGs was performed to identify enriched biological process, molecular function, and cell component. **b.** The KEGG pathway analysis of DEGs was performed using R package clusterProfiler. **c.** Volcano plot showed the down-regulated (blue) and up-regulated (red) DEGs in colonic tissue of elderly-onset UC compared with adult-onset UC. **d-f.** GSEA based on MSigDB GO (d), KEGG (e) and Reactome (f) gene sets was performed and depicted the enriched gene sets identified between adult and elderly-onset UC associated with mitochondrial function



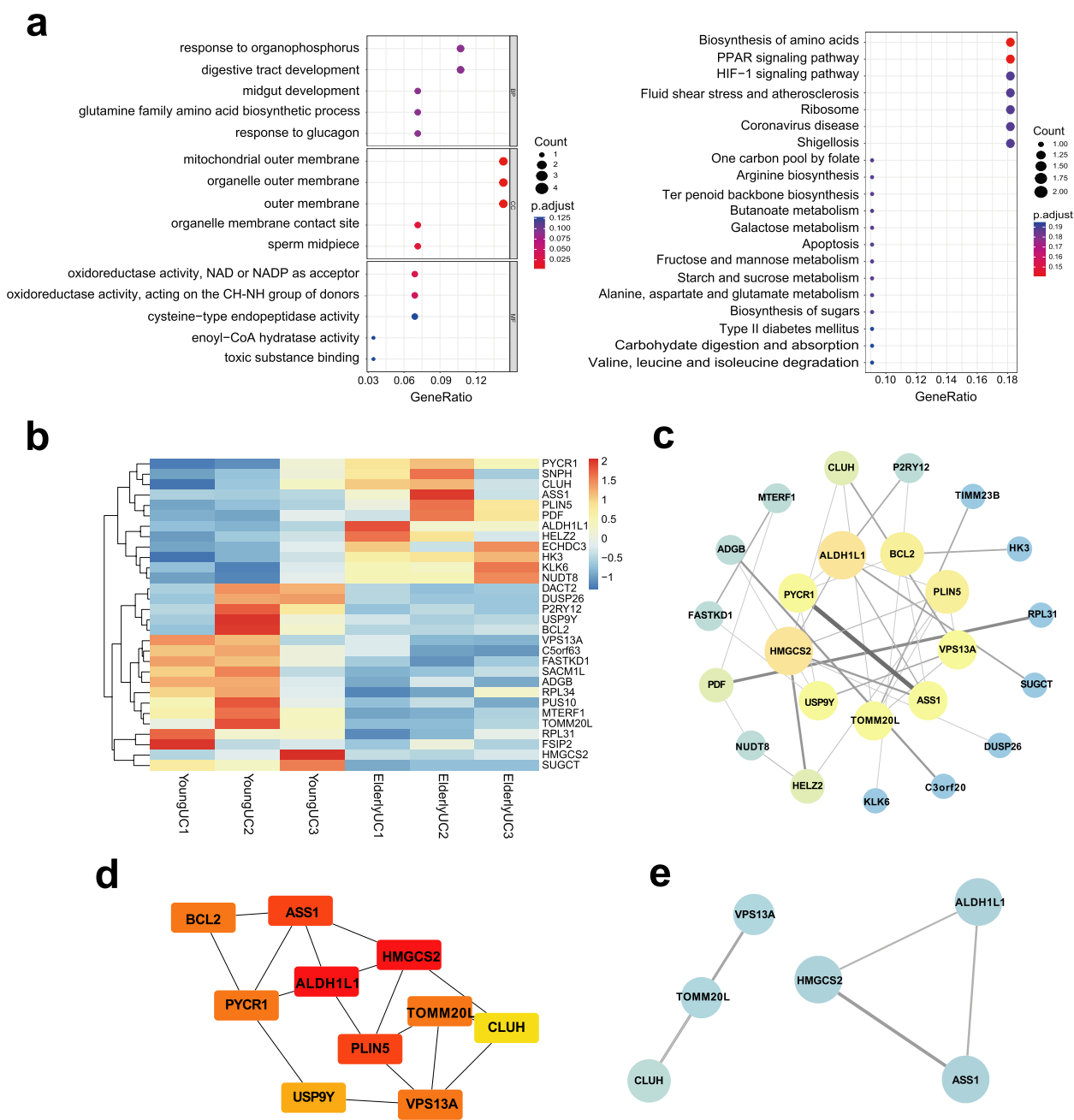


**Fig. 2** The identification, gene-set enrichment analysis and protein-protein interaction (PPI) network of mitochondria-related DEGs (mDEGs) between adult- and elderly-onset UC patients. **a.** GO and KEGG analysis of mDEGs presented the enriched mitochondria-related pathways. **b.** The heatmaps showed the differential expression of 30 mDEGs between adult- and elderly-onset UC. Each row represents a gene, and each column represents a sample. Red indicates higher expression, and blue indicates lower expression relative to the mean. **c.** The PPI network of mDEGs were performed using the STRING database. **d.** Based on the PPI network, the top 10 hub genes among mDEGs were identified using CytoHubba plugin. Red color indicates highly interactive; orange color indicates moderate interactive; yellow color indicates mild interactive. **e.** The 2 clusters identified by MCODE plugin with the highest score comprised 6 genes

the peroxisome proliferator-activated receptor (PPAR) signaling pathway, hypoxia inductive factor (HIF) 1 signaling transduction, one carbon pool by folate, etc.

PPI protein network analysis revealed that there were close interactions among mDEGs at the protein level

(Fig. 2c). As illustrated in Fig. 2d, based on the cytoHubba MCC algorithm, the top 10 hub genes were identified including *ALDH1L1*, *HMGCS2*, *PLIN5*, *ASS1*, *VPS13A*, *TOMM20L*, *PYCR1*, *BCL2*, *USP9Y*, *CLUH*. Using the

MCODE plug-in, two clusters containing six genes were identified (Fig. 2e).

### Mitochondrial abnormalities in young and aged colitis mice

After being administered 2% DSS in the drinking water, aged mice exhibited higher disease activity and histological scores than those in the young mice, as shown in Fig. 3a, b, d, and e. qRT-PCR revealed a significant increase in IL-1 $\beta$  in the colonic tissue of aged colitis mice (Fig. 3c). The average number of mitochondria per colonic epithelial cell was significantly reduced in the colitis group, and notably, mitochondrial number decreased more in aged colitis mice versus young colitis group (Fig. 3g). Consistently, TOMM20L expression, which is usually used as a surrogate for mitochondrial content, was downregulated in patients with colitis, especially more significantly in elderly UC (Fig. 4). The mitochondrial morphology of colonic mucosa in young and aged DSS colitis mice was observed via TEM (Fig. 3f), the mitochondria in the colonic epithelial cells from young control group were normal in size and shape, and the mitochondrial outer membrane and ridge were intact. The mitochondrial structure of the aged control mice was almost normal, with some swelling and shallowing of the matrix, whereas most mitochondria in the DSS-induced colitis group exhibited swelling, shallowing of the matrix and disarrangement or breaking of the mitochondrial cristae. The mitochondria in epithelial cells from aged colitis mucosa were relatively more damaged and the cristae destruction was more serious.

ATP levels were measured in colon tissues of young and aged DSS-induced colitis mice to assess mitochondrial respiratory function. As illustrated in Fig. 3h, compared with the young control group ( $41.0 \pm 9.7$  nmol/mg protein), ATP levels were decreased in the young DSS-induced colitis mice ( $37.5 \pm 9.9$  nmol/mg protein) and aged mice, most significantly in aged DSS-induced colitis group ( $24.3 \pm 6.2$  nmol/mg protein).

As mentioned above, 30 mitochondrial-related genes (*CLUH*, *SNPH*, *ASS1*, *PDE*, *PLIN5*, *TIMM23B*, *HELZ2*, *ALDH1L1*, *HK3*, *ECHDC3*, *PYCR1*, *NUDT8*, *KLK6*, *SUGCT*, *RPL31*, *TOMM20L*, *MTERF1*, *ADGB*, *PUS10*, *VPS13A*, *FASTKD1*, *C5orf63*, *CUTA*, *HMGCS2*, *BCL2*, *USP9Y*, *C3orf20*, *P2RY12*, *DUSP26*, and *DACT2*) were identified as mDEGs in the colonic mucosa of elderly and adult UC patients by RNA-seq analysis and the MitoMiner database. We further validated the mRNA expression of mDEGs and several previously reported mitochondria-related genes in human and mouse samples by qRT-PCR.

The endoscopic Mayo scores of colon biopsy sites in adult and elderly UC patients were not significantly

different. As shown in Fig. 4a and Supplementary Fig. 2, qRT-PCR revealed that there were some differences in the mRNA expression of some mitochondria-related genes between adult and elderly healthy controls. The mRNA expression of *ALDH1L1*, a hub gene, was decreased in UC patients compared with healthy controls, and its downregulation in elderly UC patients relative to elderly healthy controls was less obvious than that in adult UC patients relative to adult healthy controls. These mitochondria-related genes were also validated in young and aged colitis mice in Fig. 4b and Supplementary Fig. 3. The changes in *ALDH1L1* expression in each group of mice were consistent with the results in UC patients. Besides, combined with the fold change and significance of the RNA-seq data and gene clusters in PPT analysis, one hub gene, *ALDH1L1*, was selected for subsequent study.

### Potential mechanisms underlying mitochondrial abnormalities and inflammation

- (1) Hub molecule ALDH1L1 regulates the NLRP3/IL-1 $\beta$  pathway.

The results of the WB and qRT-PCR validation of HCT116 cells treated with siALDH1L1 are presented in Supplementary Fig. 1. ROS detection was performed in HCT116 cells transfected with siALDH1L1 and the results (Fig. 5a) showed that the mean fluorescence intensity of MitoSOX-positive in the siRNA intervention group was lower than that in the NC group after TNF $\alpha$  stimulation, suggesting that the mitochondrial ROS level in HCT116 cells decreased after ALDH1L1 expression was inhibited. The oxygen consumption rate of HCT116 cells treated with siALDH1L1 was subsequently measured to assess mitochondrial respiratory function. As shown in Fig. 5c, the basal respiration, maximum respiration, backup respiration capacity and ATP levels of the siALDH1L1 group presented increasing trends compared with the NC group. The inflammatory phenotypes of HCT116 cells after siALDH1L1 interference under exogenous TNF- $\alpha$  stimulation were measured. Similarly, as shown in Fig. 5b, WB showed that the expression of NLRP3 and IL-1 $\beta$  in the siALDH1L1+TNF- $\alpha$  group was lower than that in the NC+TNF- $\alpha$  group (both  $P < 0.05$ ). Therefore, we predict that after interfering with ALDH1L1 expression, the activation of NLRP3 and the inflammatory factor IL-1 $\beta$  were inhibited under TNF- $\alpha$  stimulation.

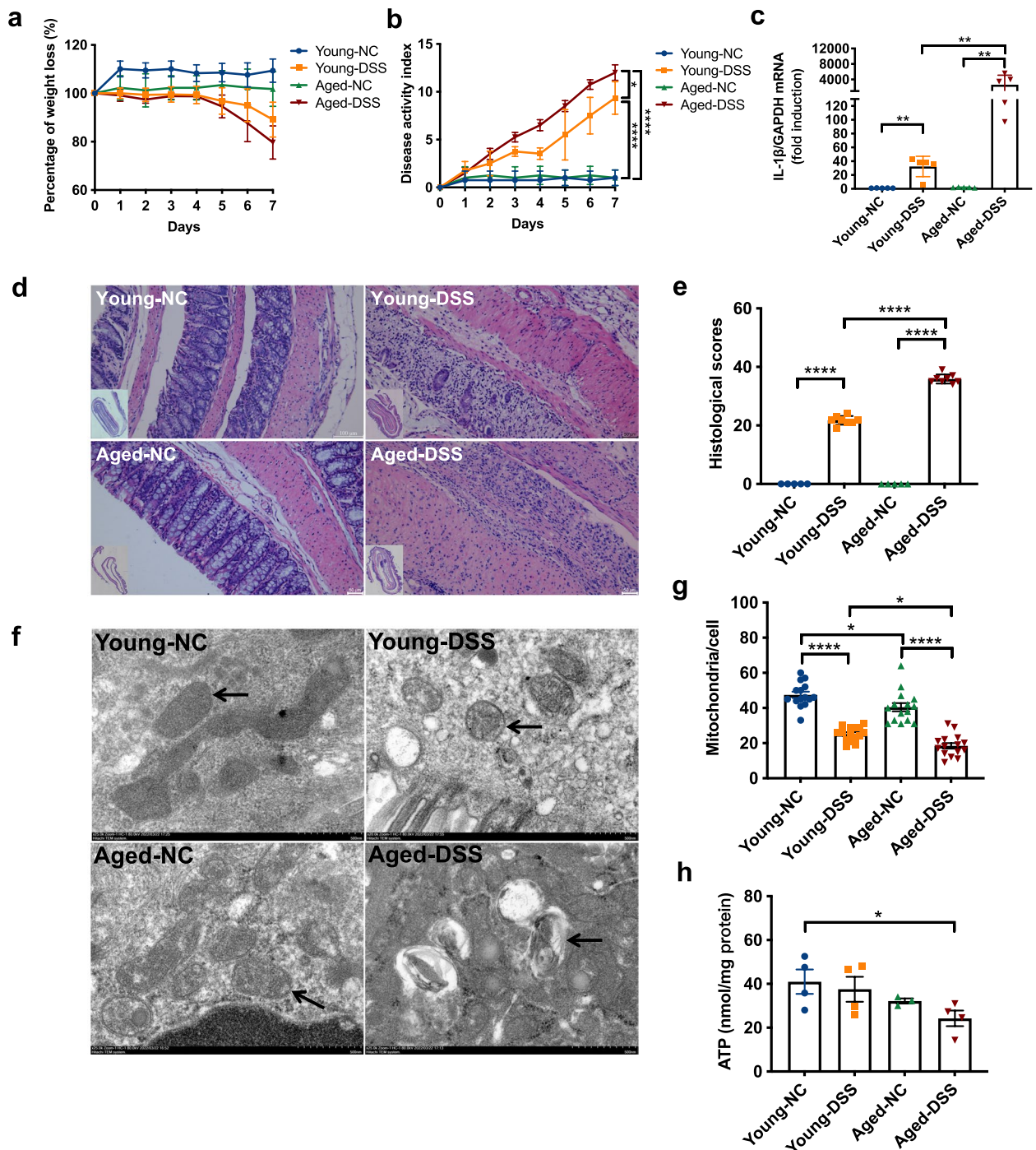


**Fig. 3** The inflammatory and mitochondrial comparison between the young and aged DSS-induced colitis mice. **a**. Body weight changes in young and aged control and DSS-induced colitis mice ( $N=5\sim 8$  mice per group). **b**. The DAI of mice during the indicated period ( $N=5\sim 8$  mice per group). Statistical significance was tested with DAI on Day 7. **c**. qRT-PCR analysis of IL-1 $\beta$  mRNA expression in colon tissues from the 4 groups ( $N=5$ ). **d**. Colonic H&E staining on Day 7 after DSS administration. Loss of crypt architecture and inflammatory cell infiltrations were both detected in colitis groups, and the aged colitis mice presented more severe. Scale bars: 50 $\mu$ m. **e**. Histological scores of the colon in each group ( $N=5\sim 8$  mice per group). **f**. Transmission electron microscopy images of murine colonic tissues, which manifested swelling mitochondria, broken or disappeared cristae, shallow matrix in colitis group, especially the aged colitis mice. Black arrows indicate the mitochondria. Scale bars: 500nm. **g**. Mitochondrial number were quantified in each group ( $N=3$ , each point indicate one randomly selected colonocyte). **h**. ATP levels were measured in colonic tissues of 4 groups ( $N=4$ ). Values were expressed as means  $\pm$  SEM. Statistical significance was determined using one-way ANOVA followed by Tukey's multiple comparisons test (b, c, e, g) or Kruskal–Wallis test (h). \* $P<0.05$ , \*\* $P<0.01$ , \*\*\* $P<0.001$ , \*\*\*\* $P<0.0001$ . Abbreviation: qRT-PCR, quantitative real-time polymerase chain reaction; SEM, standard error of the mean; DAI, disease activity index

(2) Association between mitochondria-related DEGs and differential immune microenvironment.

The compositions of 22 types of immune cells in each sample were presented in Fig. 6a and c. The results indicated that activated mast cells, resting CD4<sup>+</sup> memory T cells, M0 macrophages, M1 macrophages, CD8<sup>+</sup> T cells, plasma cells, and neutrophils were the main infiltrating immune cells. There were some significantly different infiltrates of immune cells, including NK cells, plasma cells, and T follicular helper (Tfh) cells, between adult- and elderly-onset UC patients in Fig. 6b ( $P < 0.05$ ). The correlation between immune cells and the 30 mDEGs was then evaluated (Fig. 6d). For instance, CLUH had significantly positive correlation with memory B cells, dendritic cells, activated memory T cells and  $\gamma\delta$ T cells, while NUDT8 was negatively correlated with those cells. ALDH1L1 was positively related to activated mast cells. The above correlation between immune cells and mDEGs did not occur in the young. Next, the correlation of 22 kinds of immune cells in elderly UC tissues was evaluated (Supplementary Fig. 4b). Tfh cells were positively correlated with CD8<sup>+</sup> T cells, NK cells, and plasma cells.  $\gamma\delta$ T cells were negatively related to Tregs and M1 macrophages. Neutrophils were negatively associated with activated NK cells and M1 macrophages. The correlation of immune cells in adult UC patients is illustrated in Supplementary Fig. 4a.

## Discussion

In this study, we identified that there were differences in mitochondrial morphology, ATP production, and expression of mitochondria-related molecules between elderly- and adult-onset UC patients through mucosal RNA sequencing and DSS colitis mouse model, which were also proved to be correlated with abnormal immune infiltration. At the cellular level, we observed that the hub mDEG, *ALDH1L1*, may affect inflammatory responses by regulating mitochondrial respiratory function, mitochondrial ROS, and the NLRP3/IL-1 $\beta$  pathway. These findings reveal the important role of mitochondrial dysfunction in the poor prognosis of elderly-onset UC patients and provide a potential therapeutic target

for alleviating the inflammatory progression in the aged population with UC.

Mitochondrial dysfunction is a hallmark of aging. Our study demonstrated that the role of mitochondrial damage in adult- and elderly-onset UC involves the following aspects: mitochondrial morphology, ATP production and mitochondria-related gene expression. First, mitochondrial swelling and crista fragmentation are common manifestations of mitochondrial structural damage in inflammatory lesions in IBD patients [22]. Mitochondrial shape and cristae are regulated mainly by mitochondrial fission- and fusion-related proteins, and are also affected by cell type, energy demand and metabolic status [23]. Normal mitochondrial structure is the basis of their energy metabolism function. The outer membrane of mitochondria contains various essential enzymes for metabolism. The inner membrane is folded into cristae attached by complexes of the respiratory chain and ATP synthase to drive ATP synthesis through oxidative phosphorylation (OXPHOS). Madan S et al. [23] found that longer mitochondria enhance respiratory function and increase ATP output through increased crista formation, whereas small, fragmented mitochondria have poor respiratory function. Our study revealed that the mitochondria in the inflamed tissue were shortened and swollen and the reduction or disappearance of cristae were consistent with the decrease in ATP levels in epithelial cells. Thus, it is speculated that mitochondrial decrease and damage is the structural basis for ATP reduction in epithelial cells from aged colitis mice. Of course the quantification via mitochondria-specific staining could be a more direct assessment of mitochondrial content, which needs to be explored in the future.

Energy metabolism and maintaining the ROS balance are the chief functions of mitochondria. We found that ATP levels in aged colitis tissues decreased more significantly compared with the young group. This finding is consistent with several previous studies [9, 24]. Sakamuri SS et al. [25] revealed that the OXPHOS rate of cerebral vascular endothelial cells in aged mice was lower, and their spare respiratory capacity was impaired, which made the aged group more vulnerable to injury. Moreover, in aging cells, abnormal mitochondrial

(See figure on next page.)

**Fig. 4** The mRNA expression of some mitochondria-related genes in colon tissues from UC patients and DSS-induced colitis mice. **a.** qRT-PCR analysis of the mRNA expression of mitochondria-related molecules (*HK3*, *DACT2*, *SUGCT*, *ECHDC3*, *ALDH1L1*, *TOMM20L*, *SDHA*, *NDUFS4*) in colonic tissues of adult- and elderly-onset UC patients and healthy controls ( $N = 5$ ). **b.** qRT-PCR analysis of the mRNA expression of the above molecules in colonic tissues of young and aged colitis mice ( $N = 5$ ). Values were expressed as means  $\pm$  SEM. Each sample was performed with 3 independent experiments. Statistical significance was determined using one-way ANOVA followed by Tukey's multiple comparisons test. \* $P < 0.05$ , \*\* $P < 0.01$ , \*\*\* $P < 0.001$ , \*\*\*\* $P < 0.0001$ . Abbreviation: qRT-PCR, quantitative real-time polymerase chain reaction; SEM, standard error of the mean; NC, negative control; UC, ulcerative colitis; DSS, dextran sodium sulfate

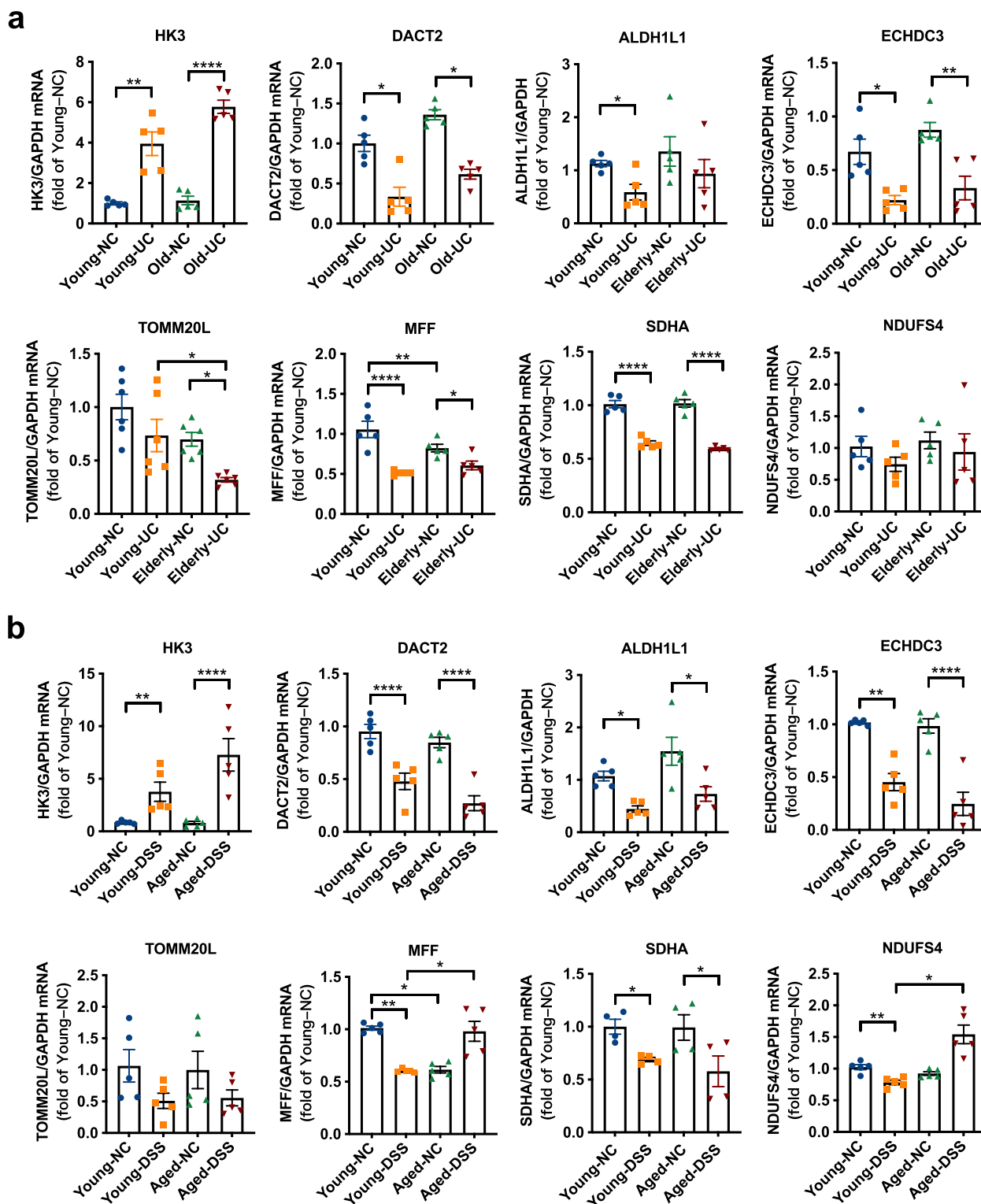


**Fig. 4** (See legend on previous page.)

structure and continued damage to electron respiratory chain will lead to excessive production of intracellular ROS, causing oxidative stress damage, which in

turn aggravates mitochondrial dysfunction in a vicious cycle and further activates multiple downstream inflammation-related signaling pathways [11]. Therefore,

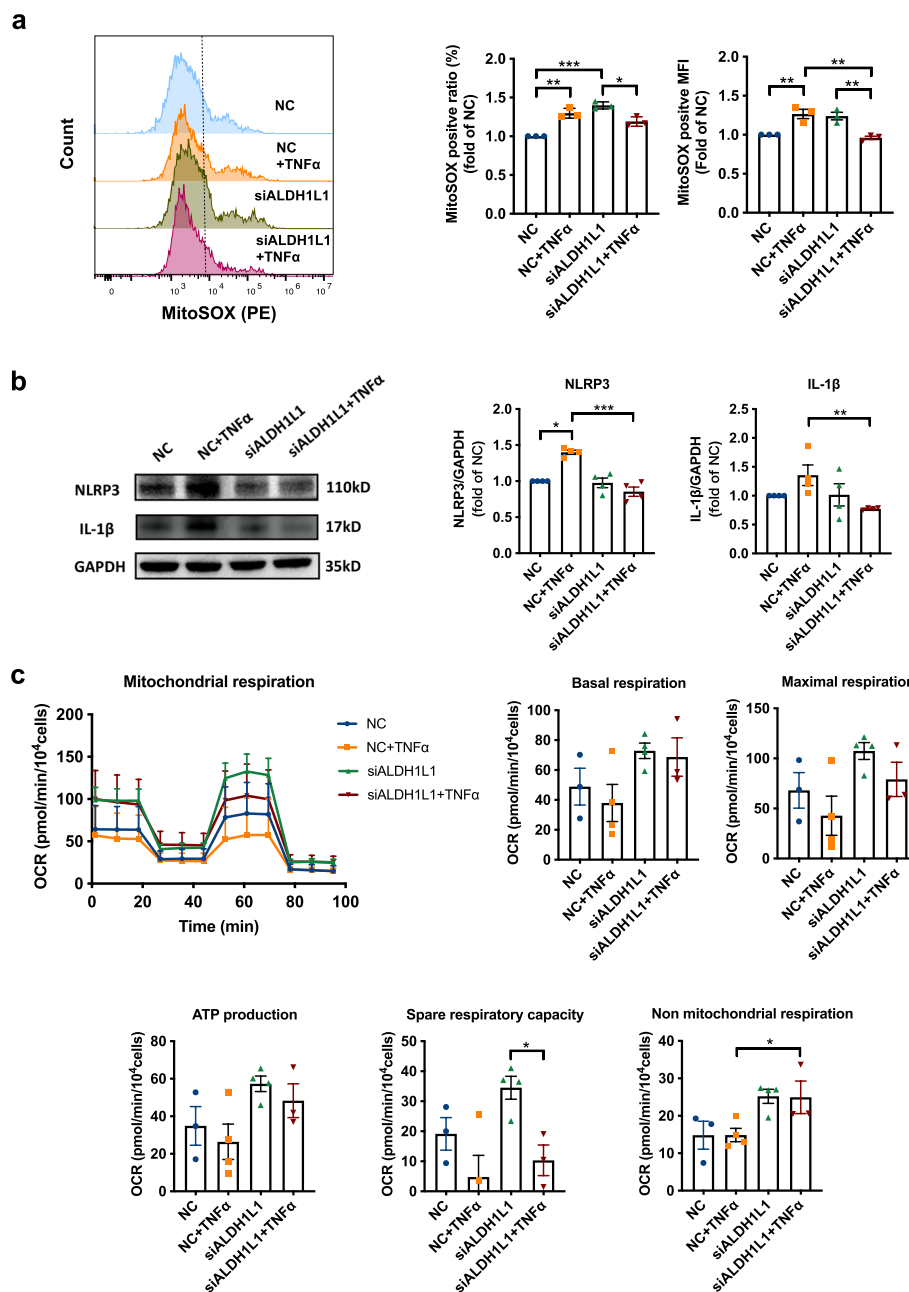


**Fig. 5** The potential mechanisms among ALDH1L1, mitochondrial dysfunction and inflammatory response. **a** Flow cytometry histograms of MitoSOX-positive HCT116 cells (left), percentage of MitoSOX-positive cells relative to NC (middle), quantification of MitoSOX-positive MFI relative to NC (right) in each group ( $N=3$ ). **b** WB showed the changes of NLRP3 and IL-1 $\beta$  in each group compared with the negative controls ( $N=4$ ). **c** The OCR measurement of each group (left). The boxplots illustrated basal respiration, maximal respiration, spare respiration capacity, non-mitochondrial respiration and ATP production in each group ( $N=3$ ). Data are mean  $\pm$  SEM of biological triplicates, and are representative of 3 independent experiments, analyzed by one-way ANOVA followed by Tukey's multiple comparisons test (a, c) or Kruskal–Wallis test (b). \* $P < 0.05$ , \*\* $P < 0.01$ , \*\*\* $P < 0.001$ , \*\*\*\* $P < 0.0001$ . Abbreviation: NC, negative control; MFI, mean fluorescence intensity; OCR, oxygen consumption rate

mitochondrial dysfunction can be an important factor contributing to a more severe inflammatory response in aged individuals.

Subsequently, some mitochondria-related DEGs were identified and validated between adult- and elderly-onset UC. Of note, RNA-seq analysis was performed in young- and elderly-onset UC with the same

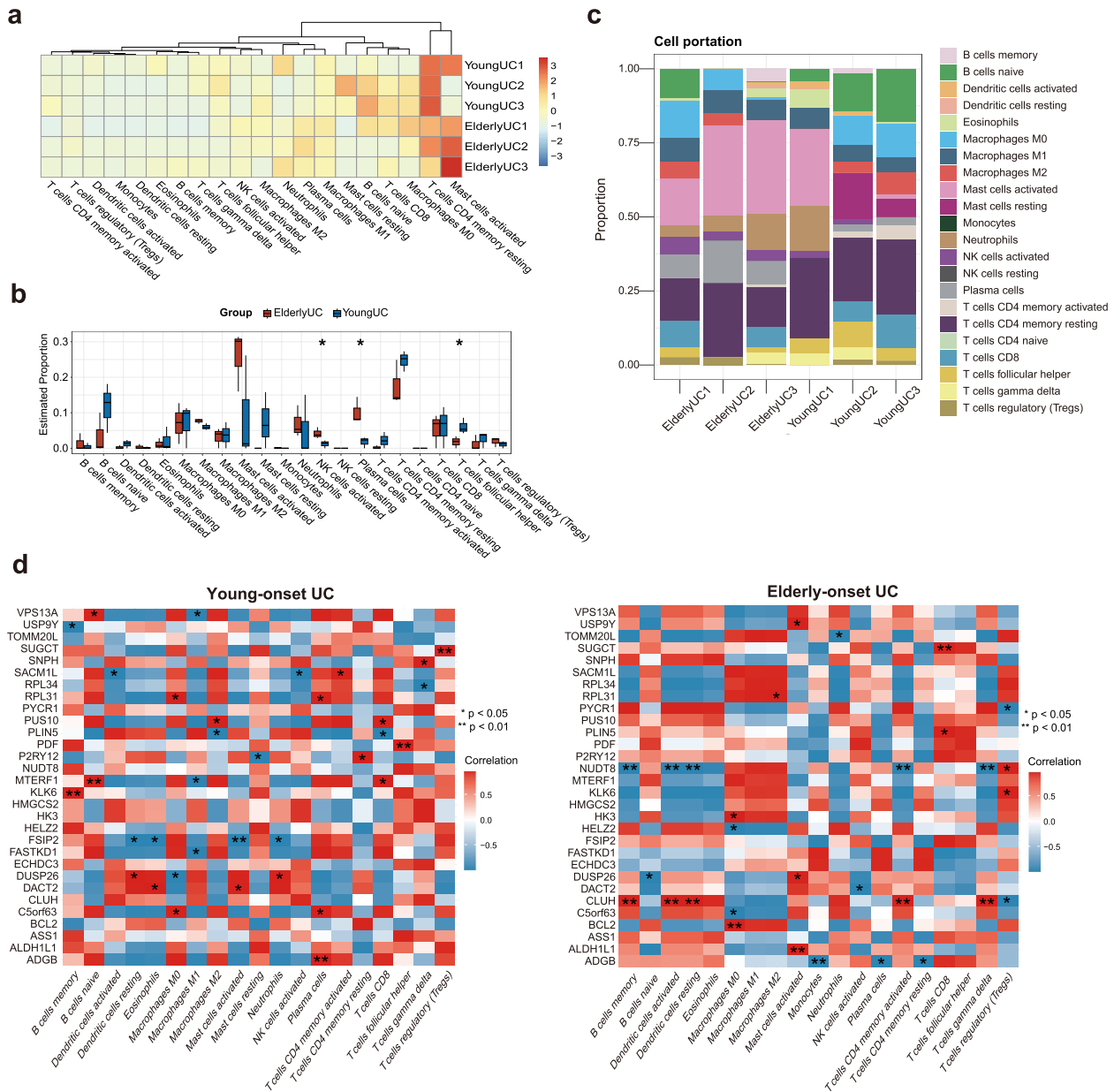


**Fig. 6** Immune cell infiltration and its relationships with mitochondria-related DEGs in colonic tissues from adult- and elderly-onset UC. **a**. The heatmap illustrating the proportions of different immune cells in each sample. Each row represents a sample, and each column represents a type of immune cell. The different color indicated the ratio of specific immune cell in this sample. Activated mast cells, resting CD4<sup>+</sup> memory T cells, M0 macrophages, M1 macrophages, CD8<sup>+</sup> T cells, plasma cells, neutrophils were the main infiltrating immune cells in the elderly UC. **b**. The boxplot showing the comparisons of immune cell profiles between adult- and elderly-onset UC tissues using the Wilcoxon test. **c**. The stacked bar plot illustrating the composition of 22 immune cell subsets in each sample. **d**. The correlation heatmap between the proportions of infiltrating immune cells and the 30 mDEGs expression in the adult- and elderly-onset UC group using Spearman's correlation analysis. Red indicated the positive correlation and blue indicated the negative correlation. Both  $N=3$  in the adult- and elderly-onset UC group. \* $P < 0.05$ , \*\* $P < 0.01$ , \*\*\* $P < 0.001$ , \*\*\*\* $P < 0.0001$

degree of activity, indicating that expression discrepancies are not secondary to different degrees of colitis but that initial changes in the elderly contribute to more severe inflammation. The differences in mDEG

expression between young and elderly healthy individuals can also partially validate this finding. In addition, although the aged DSS mice presented more severe colitis, the young and aged mice were both received

equal concentrations of DSS and their DSS intake per unit body weight, as measured by water intake, was comparable between the two groups. These findings suggest that aging itself can cause mitochondrial damage, which aggravates the vulnerability to injury and the inflammatory response. Thus, even if there is no difference in endoscopic Mayo activity, more predominant mitochondrial injury in the elderly UC may be an important factor in their greater epithelial dysfunction and slower mucosal recovery.

We found that ALDH1L1, a hub molecule that is differentially expressed in young and aged UC or DSS-induced colitis mice, played an important role in the regulation of mitochondrial functions. ALDH1L1, a member of the aldehyde dehydrogenase protein family, exists mainly in the cytoplasm and catalyzes the conversion of 10-formyltetrahydrofolate to tetrahydrofolate (THF) and CO<sub>2</sub> in the NADP<sup>+</sup>/NADPH-dependent pathway, regulating the availability of one-carbon groups for folate-dependent biochemical reactions and NADPH-dependent metabolic pathways [26, 27]. To our knowledge, most studies on ALDH1L1 have been in the oncology field and there have been no related reports about ALDH1L1 expression and inflammatory response.

We revealed that ALDH1L1 is closely related to the inflammatory process. In tissue samples, ALDH1L1 expression was significantly downregulated in the inflammatory condition, while inhibiting ALDH1L1 in colonocytes with siRNA led to a relatively mild inflammatory response under equivalent inflammatory stimuli. There seem to be some inconsistencies between *in vivo* and *in vitro* studies. We speculate that there may be some possible reasons. Firstly, downregulated ALDH1L1 expression in DSS colitis mice may be a protective feedback under inflammatory stimuli. Cellular ALDH1L1 inhibition can alleviate but not eliminate inflammation, so reduced ALDH1L1 expression in the DSS group did not alter the final inflammatory state. Then, the changes in ALDH1L1 may be affected by other molecules, as the inflammatory response or mitochondrial function is regulated by multiple factors in mice, specifically, ALDH1L1 can regulate NADPH, and the downstream network of NADPH is very extensive. The overall effect of ALDH1L1 on cellular metabolism can extend beyond immediate metabolic pathways controlled by ALDH1L1 itself [27]. There may be other mechanisms besides ALDH1L1-associated pathways involved in this process, which requires further in-depth validation. Additionally, ALDH1L1 may be influenced by phasic changes, although there is no direct evidence to support this hypothesis. Krupenko et al. [28, 29] reported that ALDH1L1 contributed to more control at a later stage of tumor progression. Likewise, inflammation is a constantly changing process, so

it cannot be ruled out that ALDH1L1 also presents phasic changes during the development of inflammation. Although not significantly different, ALDH1L1 expression in the elderly UC patients tended to increase than that in adult UC, which may explain their more severe inflammatory response and poor prognosis.

Mitochondrial dysfunction and oxidative stress imbalance mediate the crucial mechanism by which ALDH1L1 affects the inflammatory response. Our study showed that low ALDH1L1 expression can attenuate mitochondrial respiration and ROS production under inflammatory conditions, which was consistent with previous studies in the fields of cardiomyopathy, metabolic diseases, etc [30, 31]. Mechanistically, it is reasonable that ALDH1L1 can affect NADPH and is further linked to the ROS balance and ATP production [32–34]. NADPH oxidases, a major source of ROS, and antioxidant glutathione can also be affected by ALDH1L1 and change NADPH levels [33, 35].

Next, the NLRP3/IL-1 $\beta$  pathway and immune cell abnormalities may be the key steps in the regulation of colitis mediated by mitochondrial damage and ALDH1L1. We observed that lower ALDH1L1 expression in colonocytes presented less NLRP3 activation and IL-1 $\beta$  increase after TNF- $\alpha$  stimulation. Similarly, in a previous study on hepatocellular carcinoma, ALDH1L1 expression in liver tissue was proved to be closely related to multiple proinflammatory molecules, including NF- $\kappa$ B, IL-6, and chemokines [28, 29]. On the other hand, through immune infiltration analysis, the ratio of activated NK cells, plasma cells, and activated mast cells were significantly higher in the colons of elderly UC patients, while the ratio of Tfh cells was lower. Plasma cells constitute a major component of chronic inflammatory infiltrates in UC [36]. A previous study demonstrated that plasma cell infiltration in the UC mucosa was upregulated, associated with the accumulation of oxidative stress [37]. Tfh cells play important roles in B-cell activation and antibody production [38]. The generation of antigen-specific Tfh cells has been reported to be suppressed in the elderly [38, 39]. And Tfh cells can regulate IgA production, thereby participating in intestinal immune homeostasis and microbial symbiosis [38]. Therefore, these findings highlight the importance of mitochondrial dysfunction in immunologic disturbances in elderly UC patients.

From these findings in our study, we predict ALDH1L1-targeted therapy might be useful for monitoring or alleviating the “aging-inflammation progression” in UC. The ALDH1L1-targeted therapy has been reported in the fields of tumor treatment. Despite the validation in pre-clinical xenograft model, a combination treatment of gossypol (an ALDH inhibitor) with

phenformin (mitochondrial complex I inhibitor), was revealed to have potential therapeutic response to lung cancer, via the induction of cell death and ATP depletion [40]. And, it was reported that ALDH1L1 was correlated with worsened clinical outcome for patients with gastric cancer, and was a potential prognostic marker and therapeutic target [41]. However, due to the heterogeneity of ALDH1L1 in different tissues or cells, more studies are demanded to validate. On the other hand, ALDH1L1 acting substrate is 10-formyltetrahydrofolate, and further regulates folate metabolism and DNA/RNA biosynthesis. Folate metabolism can regulate the inflammatory response and oxidative stress in IBD [42, 43]. From this perspective, the combined treatment of ALDH1L1 inhibition with folic acid supplementation may be a promising therapeutic option for elderly-onset UC.

This is the first study to perform transcriptome analysis of the colonic mucosa of elderly- and adult-onset UC patients, and reveal the role of mitochondrial injury in their pathogenesis via bioinformatics analysis and further validation in DSS-induced colitis mouse model. For the first time, we offer insights into the landscape of immune cells and the correlation between mitochondrial damage and immune cell differences in young and elderly UC patients. However, there are some limits. While the OCR provides an index of ATP production, the amount of ATP produced per unit of oxygen consumed may vary greatly [44], so more assessments of mitochondrial respiration should be performed. Then, direct evaluation of mitochondrial function in the colonic tissue of UC patients was unable to be achieved because of the limited amount of tissue specimens. We did not obtain reliable results from mitochondrial function tests using primary colonocytes isolated from DSS colitis mice, as the colonocytes isolated from colitis mice, particularly the aged colitis mice, were always extremely fragile and cannot maintain stable cell viability. In addition, ALDH1L1 is an enzyme whose function may not be entirely dependent on its expression. Therefore, measurement of ALDH1L1 function is also required in subsequent work. So, in terms of sample size and mechanistic study, our evidence is still not sufficient and these questions urgently demand further investigation and exploration. The validation in normal colon epithelial cells or human primary cells will be more accurate.

In conclusion, our data suggest that there are significant discrepancies in mitochondrial morphology, ATP production and mitochondria-related gene expression between adult- and elderly-onset UC patients. Prominent mitochondrial injury may be a key factor for abnormal immunity, a more severe inflammatory response and poorer outcomes in elderly-onset UC patients. The

exploration and development of mitochondrion-targeted therapy will benefit elderly UC patients more.

#### Abbreviations

UC	Ulcerative colitis
IBD	Inflammatory bowel disease
DSS	Dextran sodium sulfate
DEGs	Differentially expressed genes
MDEGs	Mitochondria-related differentially expressed genes
ROS	Reactive oxygen species
ECCO	European Crohn's and Colitis Organization
GO	Gene Ontology
KEGG	Kyoto Encyclopedia of Genes and Genomes
GSEA	Gene set enrichment analysis
PPI	Protein-protein interaction
DAI	Disease activity index
TNF	Tumor necrosis factor
NC	Negative control
OCR	Oxygen consumption rate
OXPHOS	Oxidative phosphorylation
ALDH	Aldehyde dehydrogenase

#### Supplementary Information

The online version contains supplementary material available at <https://doi.org/10.1186/s12979-024-00494-5>.

Supplementary Material 1.

Supplementary Material 2.

#### Authors' contributions

Mengmeng Zhang: Study design, patient recruitment, experiments and analysis, drafting the manuscript Hong Lv: Study concept and design, patient recruitment Xiaoyin Bai, Gechong Ruan: Patient recruitment Qing Li, Kai Lin: Experiments and analysis support Hong Yang, Jiaming Qian: Study concept and design, experiments and analysis support, critical revision of manuscript.

#### Funding

This study was supported by National Natural Science Foundation of China (No.81970495), the National High-Level Hospital Clinical Research Funding (2022-PUMCH-C-018), the CAMS Innovation Fund for Medical Sciences (2022-I2M-C&T-B-011), National Key Clinical Specialty Project of China (ZK108000), Peking Union Medical College Hospital Research Funding for Postdoc (kyfyjj202406).

#### Data availability

No datasets were generated or analysed during the current study.

#### Declarations

##### Ethics approval and consent to participate

The ethics of this study were approved by the Ethics Committee of Peking Union Medical College Hospital.

##### Competing interests

The authors declare no competing interests.

##### Author details

<sup>1</sup>Department of Gastroenterology, Peking Union Medical College Hospital, Chinese Academy of Medical Sciences and Peking Union Medical College, Beijing, China. <sup>2</sup>Department of Pathology, Institute of Basic Medical Sciences Chinese Academy of Medical Sciences, Beijing, China.

Received: 29 July 2024 Accepted: 21 December 2024

Published online: 10 January 2025

## References

- Danpanichkul P, Suparan K, Arayakarnkul S, et al. Global epidemiology and burden of elderly-onset inflammatory bowel disease: a decade in review. *J Clin Med*. 2023;12(15):5142.
- Zhang M, Lv H, Yang H, et al. Elderly patients with moderate-to-severe ulcerative colitis are more likely to have treatment failure and adverse outcome. *Gerontology*. 2023;69(2):119–29.
- Liu A, Lv H, Wang H, et al. Aging increases the severity of colitis and the related changes to the gut barrier and gut microbiota in humans and mice. *J Gerontol A Biol Sci Med Sci*. 2020;75(7):1284–92.
- Li X, Wang C, Zhu J, et al. Sodium butyrate ameliorates oxidative stress-induced intestinal epithelium barrier injury and mitochondrial damage through AMPK-Mitophagy pathway. *Oxid Med Cell Longev*. 2022;2022:3745135.
- Ho G-T, Theiss AL. Mitochondria and inflammatory bowel diseases: toward a stratified therapeutic intervention. *Annu Rev Physiol*. 2022;84:435–59.
- Peña-Cearra A, Castelo J, Lavín JL, et al. Mitochondrial dysfunction-associated microbiota establishes a transmissible refractory response to anti-TNF therapy during ulcerative colitis. *Gut Microbes*. 2023;15(2):2266626.
- Pravda J. Radical induction theory of ulcerative colitis. *World J Gastroenterol*. 2005;11(16):2371–84.
- Haberman Y, Karns R, Dexheimer PJ, et al. Ulcerative colitis mucosal transcriptomes reveal mitochondrial pathology and personalized mechanisms underlying disease severity and treatment response. *Nat Commun*. 2019;10(1):38.
- Schneider AM, Özsoy M, Zimmermann FA, et al. Age-related deterioration of mitochondrial function in the intestine. *Oxid Med Cell Longev*. 2020;2020:4898217.
- Lee H-C, Wei Y-H. Mitochondria and aging. *Adv Exp Med Biol*. 2012;942:311–27.
- Pagan LU, Gomes MJ, Gatto M, et al. The role of oxidative stress in the aging heart. *Antioxidants (Basel)*. 2022;11(2):336.
- Meng G, Monaghan TM, Duggal NA, et al. Microbial-immune crosstalk in elderly-onset inflammatory bowel disease: uncharted territory. *J Crohns Colitis*. 2023;17(8):1309–25.
- Zhou J, Huang J, Li Z, et al. Identification of aging-related biomarkers and immune infiltration characteristics in osteoarthritis based on bioinformatics analysis and machine learning. *Front Immunol*. 2023;14:1168780.
- Ruan Y, Lv W, Li S, et al. Identification of telomere-related genes associated with aging-related molecular clusters and the construction of a diagnostic model in Alzheimer's disease based on a bioinformatic analysis. *Comput Biol Med*. 2023;159:106922.
- Magro F, Gionchetti P, Eliakim R, et al. Third European evidence-based consensus on diagnosis and management of ulcerative colitis. Part 1: definitions, diagnosis, extra-intestinal manifestations, pregnancy, cancer surveillance, surgery, and ileo-anal Pouch disorders. *J Crohns Colitis*. 2017;11(6):649–70.
- Chen B, Khodadoust MS, Liu CL, et al. Profiling tumor infiltrating immune cells with CIBERSORT. *Methods Mol Biol*. 2018;1711:243–59.
- Newman AM, Liu CL, Green MR, et al. Robust enumeration of cell subsets from tissue expression profiles. *Nat Methods*. 2015;12(5):453–7.
- Zhao H, Zhang H, Wu H, et al. Protective role of 1,25(OH)<sub>2</sub> vitamin D<sub>3</sub> in the mucosal injury and epithelial barrier disruption in DSS-induced acute colitis in mice. *BMC Gastroenterol*. 2012;12:57.
- Bialkowska AB, Ghaleb AM, Nandan MO, et al. Improved Swiss-rolling technique for intestinal tissue preparation for immunohistochemical and immunofluorescent analyses. *J Vis Exp*. 2016;113:54161.
- Rosenstiel P, Fantini M, Bräutigam K, et al. TNF-alpha and IFN-gamma regulate the expression of the NOD2 (CARD15) gene in human intestinal epithelial cells. *Gastroenterology*. 2003;124(4):1001–9.
- Speciale A, Muscarà C, Molonia MS, et al. In vitro protective effects of a standardized extract from *Cynara Cardunculus* L. Leaves against TNF- $\alpha$ -induced intestinal inflammation. *Front Pharmacol*. 2022;13:809938.
- Khaloian S, Rath E, Hammoudi N, et al. Mitochondrial impairment drives intestinal stem cell transition into dysfunctional Paneth cells predicting Crohn's disease recurrence. *Gut*. 2020;69(11):1939–51.
- Madan S, Uttekar B, Chowdhary S, et al. Mitochondria lead the way: mitochondrial dynamics and function in cellular movements in development and disease. *Front Cell Dev Biol*. 2021;9:781933.
- Martini H, Passos JF. Cellular senescence: all roads lead to mitochondria. *FEBS J*. 2023;290(5):1186–202.
- Sakamuri SS, Sure VN, Kolli L, et al. Aging related impairment of brain microvascular bioenergetics involves oxidative phosphorylation and glycolytic pathways. *J Cereb Blood Flow Metab*. 2022;42(8):1410–24.
- Krupenko SA, Krupenko NI. Loss of ALDH1L1 folate enzyme confers a selective metabolic advantage for tumor progression. *Chem Biol Interact*. 2019;302:149–55.
- Rushing BR, Fogle HM, Sharma J, et al. Exploratory metabolomics underscores the folate enzyme ALDH1L1 as a regulator of glycine and methylation reactions. *Molecules*. 2022;27(23):8394.
- Krupenko NI, Sharma J, Padiaditakis P, et al. Cytosolic 10-formyltetrahydrofolate dehydrogenase regulates glycine metabolism in mouse liver. *Sci Rep*. 2019;9(1):14937.
- Krupenko NI, Sharma J, Fogle HM, et al. Knockout of Putative tumor suppressor Aldh1l1 in mice reprograms metabolism to accelerate growth of tumors in a Diethylnitrosamine (DEN) model of liver carcinogenesis. *Cancers (Basel)*. 2021;13(13):3219.
- Wang F, Liang Q, Ma Y, et al. Silica nanoparticles induce pyroptosis and cardiac hypertrophy via ROS/NLRP3/Caspase-1 pathway. *Free Radic Biol Med*. 2022;182:171–81.
- Zhang Y, Yan M, Niu W, et al. Tricalcium phosphate particles promote pyroptotic death of calvaria osteocytes through the ROS/NLRP3/Caspase-1 signaling axis in amouse osteolysis model. *Int Immunopharmacol*. 2022;107: 108699.
- Fernandez-Marcos PJ, Nóbrega-Pereira S. NADPH: new oxygen for the ROS theory of aging. *Oncotarget*. 2016;7(32):50814–5.
- Damal Villivalam S, Ebert SM, Lim HW, et al. A necessary role of DNMT3A in endurance exercise by suppressing ALDH1L1-mediated oxidative stress. *EMBO J*. 2021;40(9):e106491.
- Oleinik NV, Krupenko NI, Priest DG, et al. Cancer cells activate p53 in response to 10-formyltetrahydrofolate dehydrogenase expression. *Biochem J*. 2005;391(Pt 3):503–11.
- Balsa E, Perry EA, Bennett CF, et al. Defective NADPH production in mitochondrial disease complex I causes inflammation and cell death. *Nat Commun*. 2020;11(1):2714.
- Scheid JF, Eraslan B, Hudak A, et al. Remodeling of colon plasma cell repertoire within ulcerative colitis patients. *J Exp Med*. 2023;220(4):e20220538.
- Mo S, Shen X, Huang B, et al. Single-cell dissection, hdWGCNA and deep learning reveal the role of oxidatively stressed plasma cells in ulcerative colitis. *Acta Biochim Biophys Sin (Shanghai)*. 2023;55:1730.
- Yu D, Walker LSK, Liu Z, et al. Targeting TFH cells in human diseases and vaccination: rationale and practice. *Nat Immunol*. 2022;23(8):1157–68.
- Silva-Cayetano A, Fra-Bido S, Robert PA, et al. Spatial dysregulation of T follicular helper cells impairs vaccine responses in aging. *Nat Immunol*. 2023;24(7):1124–37.
- Kang JH, Lee S-H, Lee J-S, et al. Aldehyde dehydrogenase inhibition combined with phenformin treatment reversed NSCLC through ATP depletion. *Oncotarget*. 2016;7(31):49397–410.
- Li K, Guo X, Wang Z, et al. The prognostic roles of ALDH1 isoenzymes in gastric cancer. *Onco Targets Ther*. 2016;9:3405–14.
- Fatahi S, Pezeshki M, Mousavi SM, et al. Effects of folic acid supplementation on C-reactive protein: A systematic review and meta-analysis of randomized controlled trials. *Nutr Metab Cardiovasc Dis*. 2019;29(5):432–9.
- Zhou D, Sun Y, Dong C, et al. Folic acid alleviated oxidative stress-induced telomere attrition and inhibited apoptosis of neurocytes in old rats. *Eur J Nutr*. 2024;63(1):291–302.
- Brand MD. The efficiency and plasticity of mitochondrial energy transduction. *Biochem Soc Trans*. 2005;33(Pt 5):897–904.

### Publisher's Note

Springer Nature remains neutral with regard to jurisdictional claims in published maps and institutional affiliations.